

1-1-2012

# An apparatus for verification of absolute calibration of quantum efficiency for charge-coupled devices

Rebecca Ann Coles  
*Wayne State University,*

Follow this and additional works at: [http://digitalcommons.wayne.edu/oa\\_theses](http://digitalcommons.wayne.edu/oa_theses)

---

## Recommended Citation

Coles, Rebecca Ann, "An apparatus for verification of absolute calibration of quantum efficiency for charge-coupled devices" (2012).  
*Wayne State University Theses*. Paper 190.

**AN APPARATUS FOR VERIFICATION OF ABSOLUTE CALIBRATION OF  
QUANTUM EFFICIENCY FOR CHARGE-COUPLED DEVICES**

by

**REBECCA COLES**

**THESIS**

Submitted to the Graduate School

of Wayne State University,

Detroit, Michigan

in partial fulfillment of the requirements

for the degree of

**MASTER OF SCIENCE**

2012

MAJOR: PHYSICS

Approved by:

---

Advisor

Date

© COPYRIGHT BY

REBECCA ANN COLES

2012

All Rights Reserved

## **ACKNOWLEDGEMENTS**

I would like to thank Professor David Cinabro for his unparalleled patience and support. I would also like to thank the research scientists and engineers at the Lawrence Berkeley National Laboratory who dedicated a great deal of their time and experience to the successful completion of my research. Most notably: Chris Bebek, John Emes, Don Groom, Sufia Haque, Steven Holland, Armin Karcher, Bill Kolbe, Julie Lee, Nick Palaio, and my advisor Natalie Roe.

I would also like to thank the Wayne State University Department of Physics and Astronomy for their dedication to my success as a physics student and researcher.

## TABLE OF CONTENTS

Acknowledgements .....	iii
Chapter 1 Introduction .....	1
Charged-Coupled Devices .....	1
Charged-Coupled Devices in Telescopes .....	1
Quantum Efficiency .....	3
Quantum Efficiency Measurement Methods .....	3
Objectives .....	5
Importance of Research .....	5
Significant Prior Research .....	6
Chapter 2 Quantum Efficiency System Setup .....	7
Light Source Section .....	7
Light Uniformity Section .....	9
Dewar and Photodiode Container Section .....	14
Voodoo Software .....	18
Chapter 3 Dewar and Photodiode Container Alterations and Functions .....	20
Construction and Assembly .....	20
Executive Summery .....	21
Scripts and Code .....	21
Chapter 4 Performance .....	28
Wavelength Calibration .....	28

Flux Calculations .....	28
Noise Measurements .....	29
Dark Current .....	29
Gain Measurements .....	30
Chapter 5 Quantum Efficiency Measurements .....	32
Quantum Efficiency versus Wavelength .....	32
Analysis Scripts .....	34
Chapter 6 System Equipment Error .....	38
Shutter .....	38
Filters .....	38
Monochromator .....	39
Sphere .....	39
Light Leaks .....	40
Total Error .....	40
Chapter 7 Conclusion .....	44
Appendix A – Parts List .....	46
Appendix B – Photodiode Container Schematics .....	47
References .....	55
Abstract .....	56
Autobiographical Statement .....	57

## LIST OF FIGURES

Figure 1: BigBOSS telescope at the Kitt Peak Observatory. Mayall Telescope photo by Pete Marenfeld, NOAO/AURA/NSF, graphic by Robin Lafever.....	2
Figure 2: Original QE measurement apparatus previous to the removal of the photodiode from the Dewar and construction of the photodiode container .....	4
Figure 3: The light source section, connected from right to left: Arc lamp, shutter, filter wheel.....	7
Figure 4: The light uniformity section, connected from right to left: monochromator, Integrating sphere, black box.....	9
Figure 5: Inside the monochromator. The beam enters from the filter wheel on the right and leaves through the slits on the upper left.....	10
Figure 6: Illustration of the monochromator's optical grating, magnified to show the individual grooves on the grating's surface. Here, 1 is the path of the incident ray and 1' is the path of the reflected ray. B is the angle of the incident ray relative to the normal of the grating, and A is the angle of the reflected ray. G is the distance between the grooves in the grating.....	11
Figure 7: Left: the interior of the black box (developed by Don Groom). The Dewar is connected on the left and a shutter connected to the integrating sphere is connected on the right. Right: compressed air delivery apparatus used to remove condensation from the window when the Dewar is cold.....	13
Figure 8: The Dewar and photodiode container section. From right to left: the Dewar and controller. Above are two Keithley Picoampmeters and two Lakeshore temperature controllers. On the left is the liquid nitrogen container that is used to fill the Dewar. Below is the vacuum pump.....	14
Figure 9: Left: the photodiode container with the photodiode in place on the rails. Right: the photodiode container connected to the Dewar window on the dark box.....	16
Figure 10: A 4k x 2k BigBOSS CCD inside the Dewar. A mask covers its picture frame style mounting to help prevent light scattering.....	17
Figure 11: Voodoo software running CCD Dewar script.....	19

Figure 12: The interior of the photodiode container and the rail system.....20

Figure 13: Volume dark current indicates the dark current through the entire bulk of the CCD, and surface dark current refers to the dark current generated on the CCD's surface. Both show the dark current as a function of temperate for BigBOSS CCDs.....30

Figure 14: image of x-ray events in a BigBOSS 4k x 2k CCD.....31

Figure 15: QE versus wavelength of a tin 500um 4k x 2k backside-illuminated CCD (ID#: 145912.4.3) measured at 140K.....34

Figure 16: QE versus wavelength of a tin 500um 4k x 2k backside-illuminated CCD (ID#: 145912.4.3). The measurements were repeated at various temperatures to show the temperature dependence of the QE. A 250um CCD is also included to show the dependence on CCD thickness in the red end of the spectrum.....34

Figure 17: QE versus wavelength of the 10mm photodiode in the photodiode container.....37

Figure 18: Monitoring correction current versus wavelength.....40

Figure 19: Four sequential measurement runs performed sequentially on a backside-illuminated LBNL CCD (ID#: 127299.3.9). The CCD temperature was held constant at 140K for each run.....42

Figure 20: Deviation from the mean QE for four sequential measurement runs performed sequentially on a backside-illuminated LBNL CCD (ID#: 127299.3.9). The CCD temperature was held constant at 140K for each run.....43

## **CHAPTER 1 INTRODUCTION**

### **CHARGE-COUPLED DEVICES**

When electromagnetic energy (such as visible light) hits matter, there is a chance the energy will be absorbed and cause the matter to emit an electron. This is called the "photoelectric effect", a process that Einstein was the first to offer a complete mathematical description of in 1905. At AT&T Bell labs in 1969, Willard Boyle, George Smith, and Michael Tompsett realized that they could collect the emitted electrons inside of bins on a silicon surface and transport them from bin to bin like a bucket-brigade to a collector that would turn the packets of electrons into a digital value that could be read and interpreted. Today, the bins are referred to by their more modern name: pixels (J. Janesick, 2001).

### **CHARGE-COUPLED DEVICES IN TELESCOPES**

Even the earliest CCDs used for astronomical observation in the 1970s were 100 times more sensitive to detecting astronomical objects than photographic plate or tube-type detectors. Because CCD's are a digital device, their images are easier to quantify and understand than for photographic plate images, leading to more reliable uncertainties. Also, without the need to develop images, as was necessary with photographic plates, more data can be produced in a much shorter period of time, making CCDs the current standard detectors for large scale telescopes.

The CCDs I tested will be used on the BigBOSS project at the Kitt Peak Observatory telescope shown in Figure 1. The purpose of BigBOSS is to measure the expansion rate of the universe by using both the baryon acoustic oscillations and redshift space distortions traced by the large scale galaxy and gas distribution. The spectral data collected from the BigBOSS

experiment is meant to be the spectroscopic counterpart to current and planned wide field imaging surveys, and will eventually be used to calculate relative distances between galaxies (LBNL BigBOSS White Paper, 2009). This data will be used to further research into the existence and nature of dark energy.

The CCDs produced at LBNL for the BigBOSS project contain  $4000 \times 4000$   $15\mu\text{m}$  pixels. The current focal plane design will contain 40 CCDs of this type. This mosaic will be capable of precisely measuring the spectra of 5,000 galaxies or stars simultaneously. Over a five year period, the CCDs will observe over 50 million objects and find precise locations for over 20 million galaxies and quasars. The map that will be generated using this data will encompass 10 times the volume of the current best map of the universe.

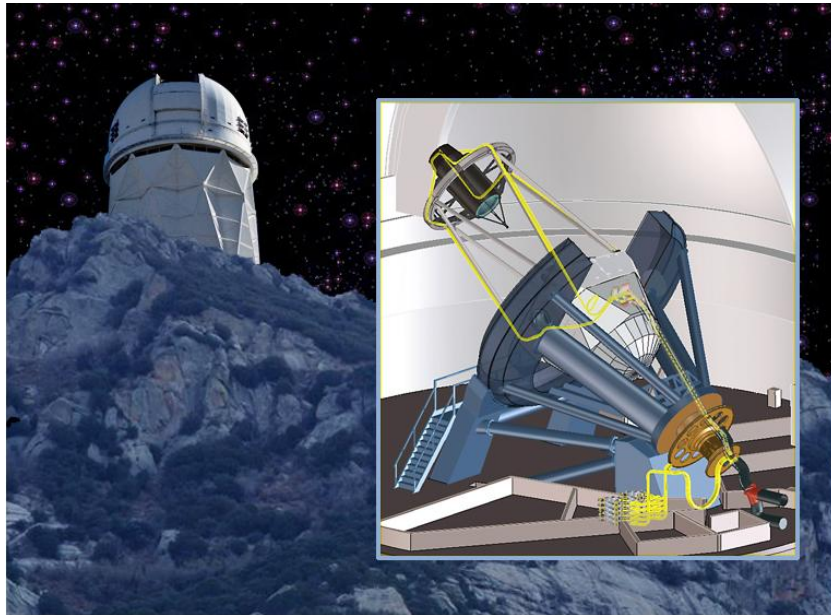


Figure 1: BigBOSS telescope at the Kitt Peak Observatory. Mayall Telescope photo by Pete Marenfeld, NOAO/AURA/NSF, graphic by Robin Lafever

## QUANTUM EFFICIENCY

Quantum efficiency is the percentage of electrons that are emitted from the CCD surface per amount of light that it's exposed to. In other words, it's the percentage of photons hitting a photo-reactive surface that are absorbed and succeed in producing electron-hole pairs. In the case of telescopes, the QE parameter is paramount in determining the accuracy of the generated images. It is valuable to know how much of the light from a galactic object was successfully captured by the CCD and is represented in the associated image.

The QE of a CCD depends on temperature, intensity of the incident light, and the wavelength of the light. Since the light from galactic objects comes in a wide range of wavelengths, a CCD's QE wavelength dependence is used as a figure of merit. Because of this, a CCD's temperature and the intensity of the light is kept constant throughout QE measurements.

## QUANTUM EFFICIENCY MEASUREMENT MEETHODS

In the QE measurement system, a calibrated photodiode is used to determine the photon flux incident on the CCD and compared to the number of electrons photo-electrically emitted and converted to signal by the CCD. The QE of a CCD is partially dependent on its geometry, material, and architecture. For a silicon CCD, the wavelengths in which the CCD is able to emit electrons in response to light is usually between 300nm to 1200nm, thus, the LBNL QE apparatus takes measurements within that range. This range was selected because high energy photons, wavelengths below 300nm, have a very short absorption length and risk being absorbed before penetrating the silicon. Lower energy photons, wavelengths above 1200nm,

have a long absorption length and tend to pass through the CCD, thus making the CCD effectively transparent to such wavelengths.

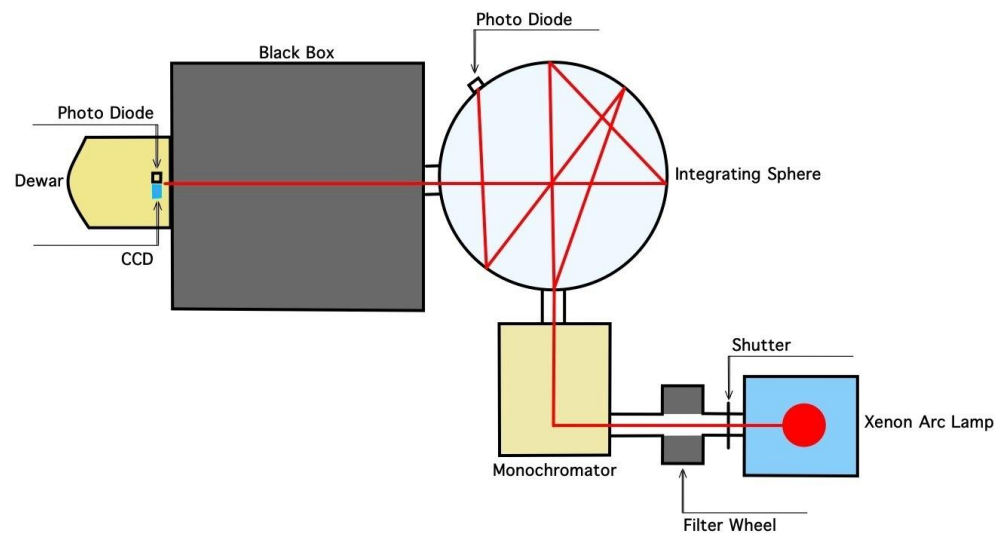


Figure 2: Original QE measurement apparatus previous to the removal of the photodiode from the Dewar and construction of the photodiode container.

The original Berkeley Lab quantum efficiency measurement system was setup up as shown in Figure 2. Light from the Xenon arc lamp is filtered to the desired wavelength by a series of bandpass filters in the filter wheel. The wavelength range of the beam is further narrowed by the monochromator before being directed into the integrating sphere. The integrating sphere converts the highly directed output beam exiting the monochromator into a homogenous diffuse source. The uniformity of the beam is influenced by the distance of the CCD from the output port of the sphere. The 80cm black box provides a drift space for the beam to achieve optimal uniformity before entering the Dewar. The Dewar is kept under

vacuum and cooled to 100K-180K depending on the operating temperature of the CCDs to be tested (J. Steckert, 2005).

### **OBJECTIVES**

The original QE system setup, with the photodiode in the Dewar next to the CCD, allowed the measurements to be independent of variations in light intensity and reflections on the glass Dewar window. My objective was to remove the photodiode from the Dewar and used a photodiode placed inside a container that connected to the current Dewar cover as the primary photodiode, with the photodiode in the integrating sphere continuing to be used as a secondary photodiode for the purpose of cross calibration and providing feedback.

### **IMPORTANCE OF RESEARCH**

The location of a photodiode in the Dewar next to the CCD, though convenient for accurate photon flux measurements, limited the size and shape of CCDs that could fit inside the Dewar. Originally, a 0.25" copper photodiode mount rested on the cold plate that also held the CCD, taking up a fair amount of space and leaving little room for a CCD mount. The location of the photodiode not only made it difficult to fit a CCD mount next to it, but also restricted the maximum size of CCD that the system can accommodate. 2"x2" CCDs, for example, required special mounts and barely fit in the small space next to the photodiode. Therefore, the LBNL Microsystems Laboratory expressed a desire to re-engineer the QE system to accommodate a greater variety of CCD sizes with minimal CCD mount adjustments. I solved this by moving the photon flux calibration to a separate container that mimicked the conditions of the Dewar.

Currently, 4k x 4k (3.4" x 3.4" picture frame mount) backside illuminated CCDs for the BigBOSS project have been successfully tested and fit within the given Dewar space with room to spare.

### **SIGNIFICANT PRIOR RESEARCH**

Three former graduate students contributed greatly to the development of the LBNL QE system: Jens Steckert who designed and constructed the QE system, Maximilian Fabricius who designed the QE system's reflectometer as well as developed various software additions, and Joanne Daniels who implemented a solution to remove condensation on the inside of the Dewar window by enhancing the temperature control methods. Also involved were various other LBNL scientists and engineers: Donald Groom, William Kolbe, Armin Karcher, etc. Jens noted in his thesis that moving the photodiode to the beam line outside of the Dewar was theoretically possible if the current system was re-engineered to support it (J. Steckert, 2005).

## CHAPTER 2 QUANTUM EFFICIENCY SYSTEM SETUP

### LIGHT SOURCE SECTION

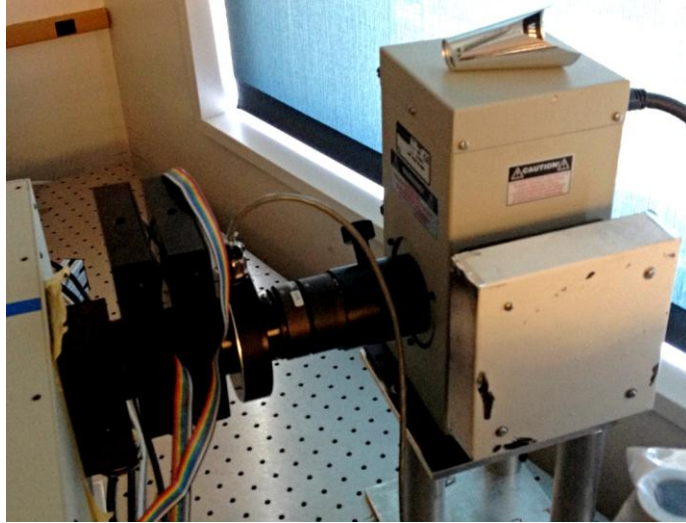


Figure 3: The light source section, connected from right to left: Arc lamp, shutter, filter wheels.

Lamp (Newport 100W Xenon Bulb, Model 6257): The wavelength range of the xenon bulb in the arc lamp shown in Figure 3 extends from 300nm to 1200nm. This simulates the blue to red spectrum that will be experienced by the CCD's when used in telescopes. Due to the pressure broadened emission lines of xenon, between 800nm and 1000nm, the intensity can be up to 30 times brighter than at other wavelengths. To correct for this, the monochromator adjusts a series of vertical slits that alter the intensity of the beam and keep it constant regardless of the wavelength. My software creates a slitwidth file that records the widths of the slits inside the monochromator and applies them to both the photodiode container measurements as well as the CCD measurements. This is described in greater detail in the monochromator section.

Shutter (Vincent Associates via Uniblitz VS25s2zM0R1 shutter, Uniblitz VMM-T1 shutter driver/timer): To control the exposure time of light on the CCD, the beam is interrupted by a shutter that sits just outside the arc lamp housing. The double-overlapping blades provide a high speed, light tight system. Average exposure times are between 1 to 30 seconds, and are determined based on the light intensity to prevent over or under exposure. I, therefore, take test images prior to each QE measurement to determine an acceptable exposure time.

A reflective coating on the shutter's blades facing the lamp provides very tight light suppression when the blades are closed to prevent light leaks. The shutter is driven by a Leach controller, the standard CCD controller at LBNL, which operates the CCD and is controlled by Voodoo software, which is discussed in greater detail in the Voodoo software section.

Filters: To reduce stray light and avoid second order effects from the monochromator, a filter wheel containing two bandpass and two longpass filters sits between the shutter and monochromator. The dielectric bandpass filters are coated with a multilayer thin film that cuts off at the transition edges.

Bandpass filter #1 transmits light between 200nm and 380nm, and bandpass filter #2 transmits light between 340nm and 475nm.

The dielectric longpass filters transmit light from the cutoff point up to more than 1200nm. Longpass filter #1 transmits light from 450nm, and longpass filter #2 transmits from 700nm.

The filter change over are controlled by the monochromator, and are as follows:

200nm - 375nm: Hoya U340 FSR-U340 (bandpass).

376nm - 475nm: Schott BG28 (bandpass).

476nm - 720nm: FLWP-450-25.0m (longpass).

721nm - 1200nm: FLWP-700-25.0m (longpass).

### LIGHT UNIFORMITY SECTION



Figure 4: The light uniformity section, connected from right to left: monochromator, integrating sphere, black box.

The light uniformity section shown in Figure 4 is designed to ensure that the light incident on the CCD is free of fluctuations in the light intensity. It is crucial that the intensity of the beam remain constant regardless of its wavelength.

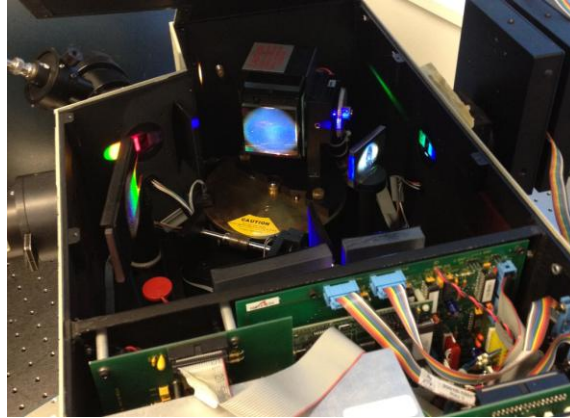


Figure 5: Inside the monochromator. The beam enters from the filter wheel on the right and leaves through the slits on the upper left.

Monochromator (Newport Model 77700): The monochromator show in Figure 5 uses the wavelength dispersion of a diffraction grating to filter light. The resulting beam has a spectral wavelength of about 10nm. The dispersion property of the grating is described by:

$$m * \lambda = g * (\sin(A) - \sin(B)) \quad (1)$$

Where  $m$  is the order (an integer),  $\lambda$  is the wavelength,  $g$  is the distance between the grooves in the grating,  $B$  is the angled of the incident ray relative to the normal of the grating, and  $A$  is the angle of the reflected ray relative to the normal of the grating as shown in Figure 6. The beam emerges from the filters and is incident on the diffraction grating. The grooves on the grating's surface spread the light as if it had originated from a series of point sources. When one wavelet's peak intersects with another wavelet's valley, they cancel each other out. Subsequently, when two wavelet's peaks intersect, they constructively interfere and the resulting wave's height is doubled. Since longer wavelength light bends more than shorter wavelength light, the angle of the grating controls which wavelength of light is aimed at the slit

opening, and therefore ensures that the wavelength of the beam exiting the monochromator is accurate to within about 10nm.

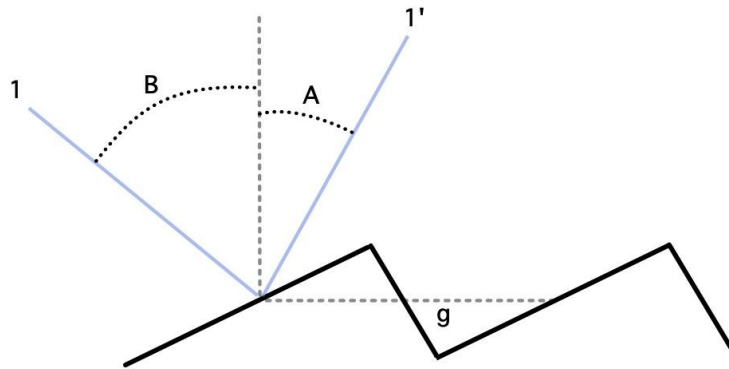


Figure 6: Illustration of the monochromator's optical grating, magnified to show the individual grooves on the grating's surface. Here, 1 is the path of the incident ray and 1' is the path of the reflected ray. *B* is the angle of the incident ray relative to the normal of the grating, and *A* is the angle of the reflected ray. *G* is the distance between the grooves in the grating.

Because the xenon bulb fluctuates in intensity around its emission lines, the monochromator adjusts the slits, closer or farther apart, at the output point to reduce the intensity, with the strongest emission line at 823nm. Slitwidth adjustments are made each time the wavelength is changed to preserve uniform light intensity throughout the measurements. Accuracy also requires that the light intensity remain constant between the photon flux measurements (photodiode container) and electron current measurements (CCD in Dewar) which are performed separately. A script records the slitwidth used for each wavelength by the monochromator and generates a table during the photodiode container measurements that is then used during CCD Dewar measurements. This preserves the intensity and wavelength accuracy between the separate measurement runs. As an extra precaution, the reading of the

photodiode inside of the integrating sphere records fluctuations in the light intensity between the runs, which is used to calculate a monitoring correction current that is applied to the measured currents upon analysis, which will be discussed later in this section.

Integrating Sphere: The light leaving the monochromator is monochromatic within a 10nm band but is of small diameter, not large enough to uniformly cover the surface of the CCD. The integrating sphere converts the beam to a uniform source of a larger diameter. The interior of the sphere is covered with a diffuse reflective film, and light entering the input port is reflected repeatedly before leaving through the output port. The multiple reflections diffuse the light so that the beam exiting the sphere is uniformly distributed.

Among other factors, the uniformity of the light leaving the sphere is determined by the port-fraction:

$$f = \frac{A_{ports}}{A_{sphere}} \quad (2)$$

The ratio of the areas of the ports and reflective surface determines the sphere size needed to create a beam of a given diameter. The diameter of the input port is 50mm, the output port is 100mm, and the diameter of the sphere is 50cm. The sphere, therefore, diffuses a 100mm diameter beam into the dark box that it connects to.

Reference diode (calibrated silicon Hamamatsu 2281: 100mm<sup>2</sup>): The integrating sphere also contains a reference diode that records the photon flux inside the sphere during both the photodiode container measurement and the CCD Dewar measurement discussed in the Dewar and Photodiode Container section. The values are used to calculate a monitoring correction

current that is multiplied by the currents to account for fluctuations in the light level between the measurements:

$$C = \frac{I_{ccd}}{I_{diode}} \quad (3)$$

Where the photodiode current measured during the photodiode container measurements is divided by the current measured during the CCD Dewar measurements. My scripts calculate and apply the monitoring correction current for every wavelength measured.

Black Box: The uniformity of the incident light is partially dependent on the distance from the output port of the sphere to the CCD. The 80cm drift space shown in Figure 7, connects the integrating sphere with the Dewar section. I added a pressurized air release tube that sits next to the Dewar window to remove the condensation that forms when the Dewar is cold.



Figure 7: Left: the interior of the black box (developed by Don Groom). The Dewar is connected on the left and a shutter connected to the integrating sphere is connected on the right. Right: compressed air delivery apparatus used to remove condensation from the window when the Dewar is cold.

## DEWAR AND PHOTODIODE CONTAINER SECTION

The photon flux and CCD current are measured separately. The photodiode container is attached to the Dewar window which is connected to the black box. The photodiode in the container measures the photon flux incident through the window for a given set of wavelengths. The photodiode container is then removed from the window and the back end of the Dewar is connected. The CCD inside the Dewar is vacuum sealed, cooled, and exposed to the same incident wavelengths as the photodiode, as shown in Figure 8. The associated current is used in conjunction with the photon flux to calculate the quantum efficiency of the CCD.



Figure 8: The Dewar and photodiode container section. From right to left: the Dewar and controller. Above are two Keithley Picoampmeters and two Lakeshore temperature controllers. On the left is the liquid nitrogen container that is used to fill the Dewar. Below is the vacuum pump.

Photodiode container: I designed the photodiode container to replicate the interior dimensions and environment of the Dewar. The container is made of 1.5" aluminum pipe, with an 11" outer diameter and 8" inner diameter. A calibrated silicon Hamamatsu S1337-1010BQ photodiode rests on a set of black anodized aluminum rails in the container's interior that can be adjusted to move the photodiode to the same relative position that the CCD will sit inside the Dewar. Thus, the distance of the beam in the drift space is the same for the photodiode as it is for the CCD.

The inside of the container is painted matte black to avoid internal reflection. This prevents scattered photons from getting a second chance to be absorbed by the CCD by reflecting off the aluminum and hitting the CCD multiple times. Since the QE of the photodiode is sensitive to temperature, the photodiode's mounting plate is temperature controlled by a Lakeshore temperature controller and a Peltier cooler that sits directly behind the photodiode as shown in Figure 9. The Dewar window connects to the dark box, and can be connected to either the photodiode container or Dewar without having to be removed. This helps decrease exposure of the Dewar window to dust and debris that could scatter incoming light. The window is also regularly cleaned.

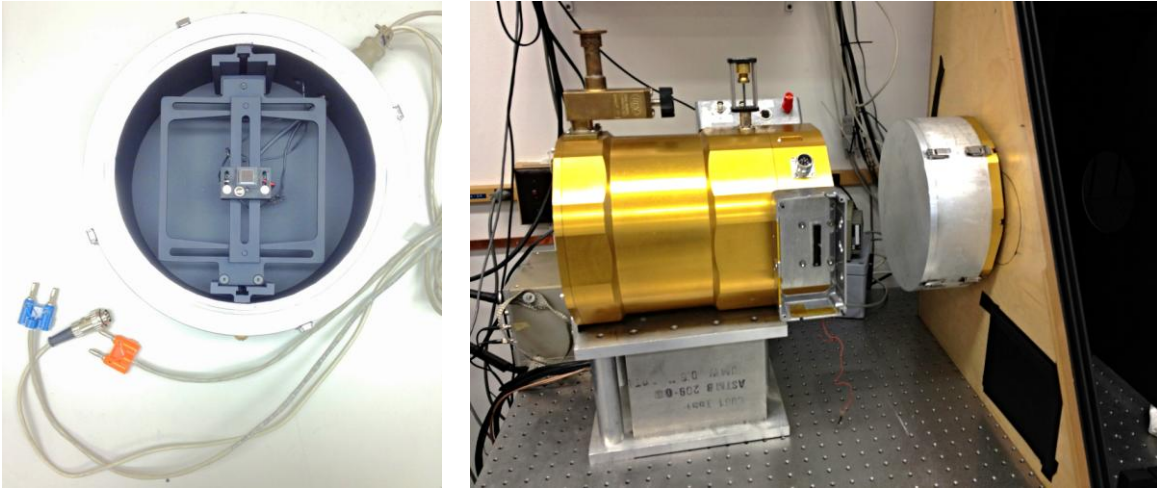


Figure 9: Left: the photodiode container with the photodiode in place on the rails. Right: the photodiode container connected to the Dewar window on the dark box.

Dewar: The Dewar contains the CCD and readout components. I vacuum seal it to  $5 \times 10^{-5}$  torr and cool it, via liquid nitrogen, to the specified operating temperature of the CCD. Since the QE and dark current of the CCD is temperature dependent, most of the LBNL backside illuminated CCD's operate around 140K. The CCD sits against the cold plate that connects via a cold strap to the liquid nitrogen tank in the back of the Dewar as shown in Figure 10. To keep the CCD temperature from fluctuating, a 50ohm resistor connected to a Lakeshore temperature control unit is connected to the back of the plate.

To help prevent stray light from reflecting off surfaces surrounding the CCD, a black anodized aluminum mask that is slightly larger in diameter than the Dewar window, is mounted in front of the CCD. I made a variety of masks to fit over the active areas of both 4k x 2k and 4k x 4k BigBOSS CCDs.

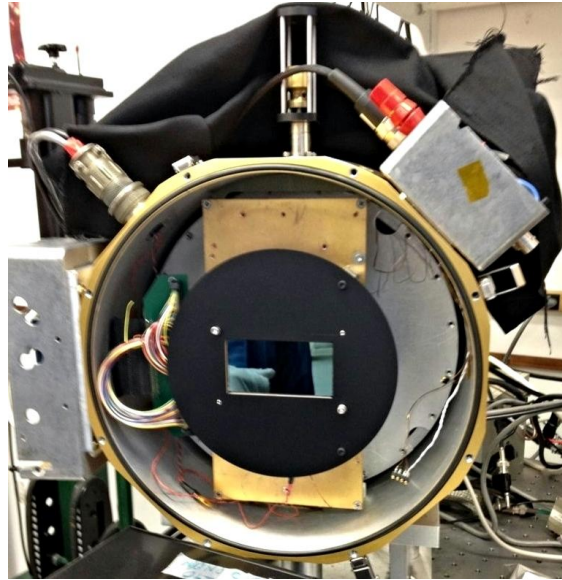


Figure 10: A 4k x 2k BigBOSS CCD inside the Dewar. A mask covers its picture frame style mounting to help prevent light scattering.

Keithleys (6483 Picoammeter): I use Keithley Picoammeters to take current measurements from the sphere and container photodiodes. The Keithleys take 20 current measurements per exposure and return the average to the Voodoo software.

Lakeshore (Auto-tuning temperature controllers: model 321, connected to 50ohm resistors): I use Lakeshore temperature controllers to maintain temperature stability of the photodiode in the container and CCD. The controllers connected to 50ohm resistors that heat the units and sensors that continuously monitor the temperature.

Controller: The Astronomical Research Cameras Inc. Leach controller and video boards control the settings, timing, and data accusation from the Lakeshores and Keithleys. The controller directly communicates with the Voodoo software.

## **VOODOO SOFTWARE**

The Voodoo software handles the automation of all mechanical components and measurements in the QE system, including: Keithleys, Lakeshores, the controller, the arc lamp, the monochromator, and both shutters as shown in Figure 11.

The software was developed by Astronomical Research Cameras Inc., but the current version 1.7.2.3.1 has since been altered by LBNL. Voodoo is written in JAVA and allows control of the QE system via scripts.

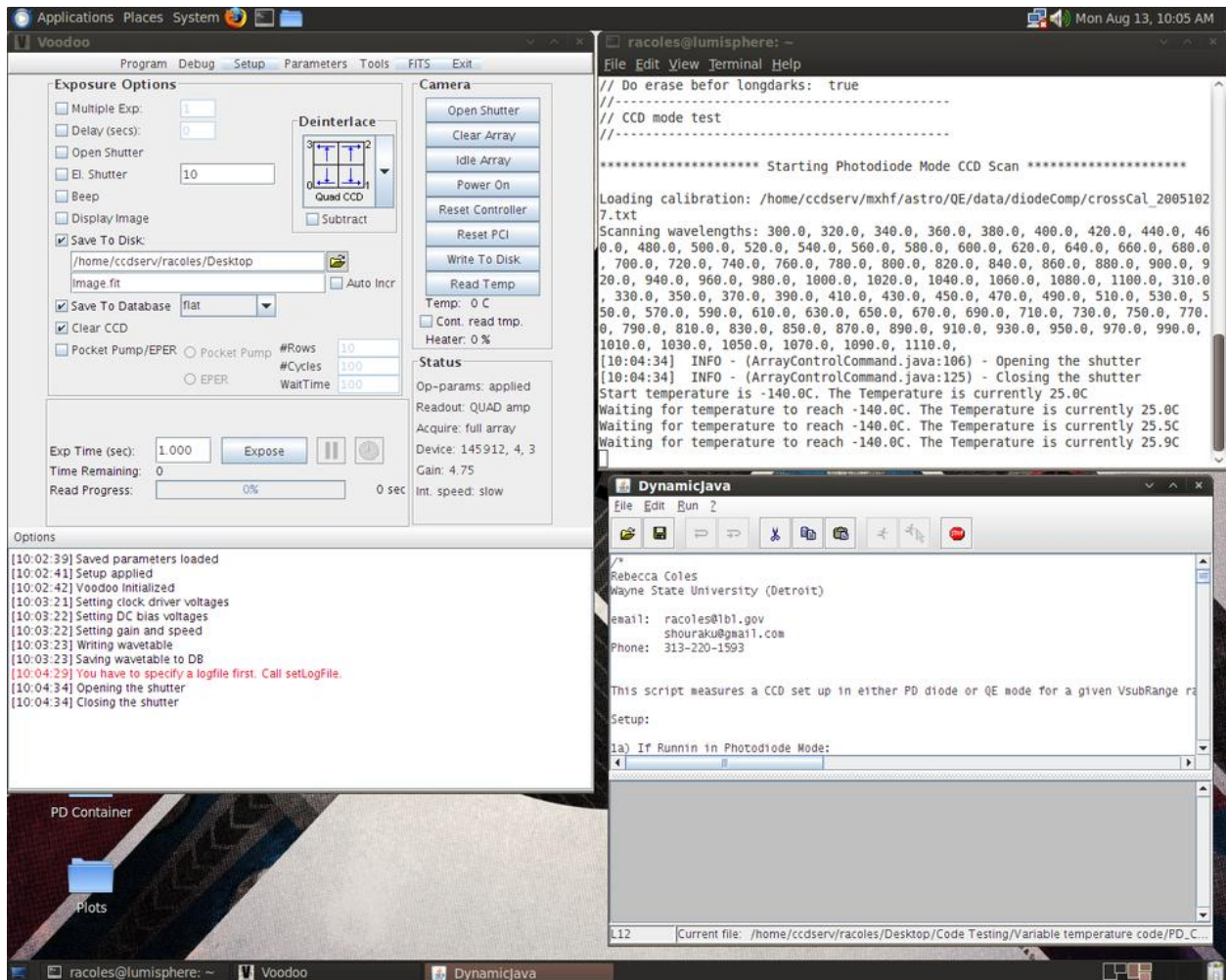


Figure 11: Voodoo software running CCD Dewar script.

### CHAPTER 3 DEWAR AND PHOTODIODE CONTAINER ALTERATIONS AND FUNCTIONS CONSTRUCTION AND ASSEMBLY

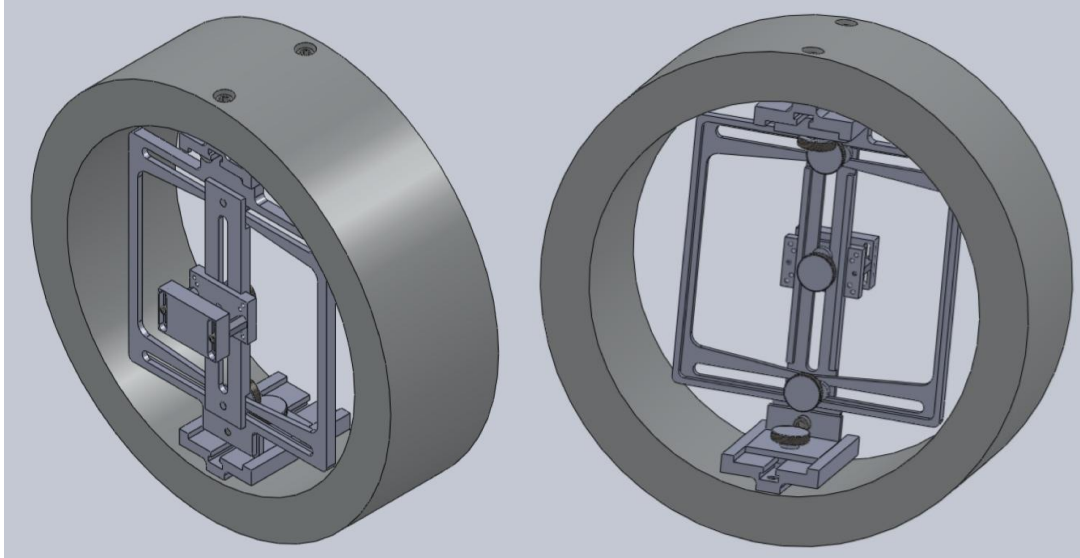


Figure 12: The interior of the photodiode container and the rail system.

As described in chapter 1, I removed the photodiode that is used for photon flux calculations from the Dewar and installed it in a container built to replicate the Dewar's architecture. The removal of the photodiode made room for larger CCDs than previously. To preserve the accuracy of the measurements, it is essential that the photodiode and CCD are exposed to the same lighting conditions. The photodiode container has the same internal dimensions as the Dewar and is anodized black using the same process and equipment as the CCD masks in the Dewar, thus replicating the level of reflection suppression as shown in Figure 12. Because the distance between from output port of the integrating sphere influences the uniformity of the diffuse beam, the photodiode is moved to the relative location of the CCD inside the Dewar by the rails.

## EXECUTIVE SUMMARY

The old QE system took photon flux and CCD current measurements simultaneously. Since the photodiode is now in the photodiode container, the photon flux measurements and CCD current measurements are taken separately. The measurement procedure is as follows: I attach the photodiode container to the Dewar window that is mounted on the black box and take photon flux measurements over a given series of wavelengths, usually every 10nm from 300nm to 1200nm. Then, I remove the container and connect the Dewar, containing the CCD, to the Dewar window. I then vacuum seal and cool the Dewar using liquid nitrogen, to the operating temperature of the CCD. I take CCD current measurements over the same wavelengths, and with the same light intensity, as I did with the photodiode. I combine the resulting data and use it to calculate the CCD's QE.

## SCRIPTS AND CODE

The automation of the QE measurements is executed by the Voodoo software via JAVA scripts. The addition of the photodiode container to the system required that new scripts be written to divide photon flux and CCD current measurements into two parts: the photodiode container script, and the Dewar/CCD script.

Photodiode Container script:

The photodiode container script operates the system as follows:

- Sets the Lakeshore to temperature control the photodiode (298K).
- Loads and applies the photodiode calibration data (provided by the manufacturer).

- Exercises the shutters to make sure that they are functioning properly.
- Sets up log and slitwidth files.
- Monitors the Lakeshore until the starting temperature is reached.
- Applies all the necessary timing delays for the system.
- Zero corrects the Keithley Picoammeters.
- Controls the lamp, turning it on if it isn't already.
- Begins the scanning loop. The loop takes measurements for all the wavelengths specified in the parameter section of the code:
  - Turns on the digital exposure control (flux control).
  - Checks the position of the filters in the filter wheel.
  - Tells the monochromator what wavelength to adjust to.
  - Tells the monochromator to perform a light level adjustment and records the associated slitwidth to a file that will later be used by the Dewar/CCD script to set the light intensity (section 3.3.2).
  - Sends the commands to take the first dark measurement: closes the shutter, arms the Keithleys, tells the Keithleys to take current measurements from the container and sphere, averages and records the current data.

-Sends the commands to take the exposed measurement: opens the shutter, arms the Keithleys, tells the Keithleys to take current measurements from the container and sphere, averages and records the current data.

-Sends the commands to take the second dark measurement using the same method as the first.

-After all specified wavelengths are measured, the command is sent to turn off the lamp in preparation for the removal of the photodiode container and installation of the Dewar.

Dewar/CCD script:

The Dewar/CCD script controls both photodiode and imaging mode. Among other parameters, the user is asked to select which mode they will be running the system in. The script is set up to repeat measurements over a set wavelength range for multiple temperature settings. In other words, the script performs the specified measurements at, say: 140K, 160K, and 180K. A full set of measurements is performed at the lowest temperature first, and then heated to the next highest and so on.

If photodiode mode is selected, the Dewar/CCD operates the system as follows:

-Sets the Lakeshore to temperature control the CCD.

-Loads and applies the photodiode calibration data (provided by the manufacturer).

-Exercises the shutters to make sure that they are functioning properly.

- Sets up a log file and loads the slitwidth file from the photodiode container scan.
- Monitors the Lakeshore until the starting temperature is reached.
- Applies all the necessary timing delays for the system.
- Zero corrects the Keithley Picoammeters.
- Controls the lamp, turning it on if it isn't already.
- Begins the scanning loop. The loop takes measurements for all the wavelengths specified in the parameter section of the code:
  - Turns on the digital exposure control (flux control).
  - Checks the position of the filters in the filter wheel.
  - Tells the monochromator what wavelength to adjust to.
  - Tells the monochromator to set the slitwidth to the value given in the slitwidth file for the specified wavelength.
  - Sends the commands to take the first dark measurement: closes the shutter, arms the Keithleys, tells Keithleys to take current measurements from the CCD in the Dewar and the photodiode in the sphere, averages and records the individual current data.
  - Sends the commands to take the exposed measurement: opens the shutter, arms the Keithleys, tells Keithleys to take current measurements from the CCD in

the Dewar and the photodiode in the sphere, averages and records the individual current data.

-Sends the commands to take the second dark measurement using the same method as with the first dark.

-After all specified wavelengths are measured, a command is sent to the Lakeshore to raise the CCD's temperature to the next given value. Once all the temperature measurement runs are complete, the script sends the command to turn off the lamp.

If imaging mode is selected, the Dewar/CCD operates the system as follows:

-Sets the Lakeshore to temperature control the CCD.

-Loads and applies the photodiode calibration data (provided by the manufacturer).

-Exercises the shutters to make sure that they are functioning properly.

-Sets up a log file and loads the slitwidth file from the photodiode container scan.

-Monitors the Lakeshore until the starting temperature is reached.

-Applies all the necessary timing delays for the system.

-Tells the controller to set the CCD substrate voltage as specified in the parameters.

-Zero corrects the Keithley Picoammeters.

-Controls the lamp, turning it on if it isn't already.

- Performs the initial CCD erase to clear the CCD, its amplifiers, and its electronics, of current prior to exposure.
- Performs an Epurge (sets the CCD clock cycles).
- Cycles the CCD clocks.
- Takes initial X-ray measurements to be used for calculate the gain during analysis.
- Begins the scanning loop. The loop takes measurements for all the wavelengths specified in the parameter section of the code:
  - Turns on the digital exposure control (flux control).
  - Checks the position of the filters in the filter wheel.
  - Tells the monochromator what wavelength to adjust to.
  - Tells the monochromator to set the slitwidth to the value given in the slitwidth file for the given wavelength.
  - Performs a second Epurge.
  - Takes an X-ray measurement.
  - Takes a dark measurement that includes a CCD image (via the controller) and sphere current measurement (via the Keithley).
  - Takes an exposed measurement that includes a CCD image (via the controller) and sphere current measurement (via the Keithley).

-Takes a longer dark measurement (long darks).

-After all specified wavelengths are measured, a command is sent to the Lakeshore to raise the CCD's temperature to the next given value. Once all the temperature measurement runs are complete, the script sends the command to turn the lamp off.

## CHAPTER 4 PERFORMANCE

### WAVELENGTH CALIBRATION

The wavelength is calibrated via the monochromator using 10nm bandpass filters. I placed the filters in front of the photodiode and used the monochromator's software to adjust the wavelength to the cutoff points of the filter. The xenon emission lines are used as they are well known, the most notable being at 823nm.

### FLUX CALCULATIONS

I calculate the photon flux per pixel by using the photodiode container measurements. The photons per square meter for a given wavelength is calculated by first finding the power generated in the CCD:

$$P = \frac{I_{exposed} - I_{dark}}{S_{photodiode}} \quad (4)$$

Where  $I$  is the current and  $S$  is the sensitivity of the photodiode. The energy per photon is:

$$E_{photon} = \frac{h * c}{\lambda} \quad (5)$$

Where  $h$  is Planck's constant,  $c$  is the speed of light, and  $\lambda$  is the wavelength. The number of photons per meter squared is:

$$\rho = \frac{P}{E} * \frac{1}{A_{photodiode}} \quad (6)$$

Where  $A$  is the area of the photodiode. The number of photons per pixel is:

$$\rho_{pixel} = \rho * A_{pixel} \quad (7)$$

Equation (7) gives the photon flux per pixel on the CCD, and is used to calculate the overall QE.

## NOISE MEASUREMENTS

The CCD's readout amplifier generates thermal noise (white noise) due to output amplifier impedance. To correct for this, I take dark measurements before and after each exposure and subtract them from the exposed image during analysis. My analysis script calculates the pixel to pixel RMS variance between the images and estimates the overall read noise. The read noise is usually about 4-20 electrons per pixel.

## DARK CURRENT

Dark current refers to the generation of electron-hole pairs in the CCD without exposure to photons. In other words, electrons that are emitted via processes other than the photoelectric effect. The LBNL CCD's are based on a p-n junction that are susceptible to reverse leakage current caused by traps within the CCD. These traps are a result of impurities in either the semiconductor or the Si-SiO<sub>2</sub> surfaces. Sometimes, electrons or their holes are excited at the trap level and are captured by the potential well in a pixel.

The dark current is a function of temperature:

$$I_{dark} = 2.5 \times 10^{15} * A_{pixel} * D_{fm} * T^{1.5} e^{-E_g/2kT} \quad (8)$$

Where  $I_{dark}$  is the average dark current in (e/sec/pixel),  $A_{pixel}$  is the area per pixel,  $D_{fm}$  is the dark figure of merit,  $T$  is the temperature,  $E_g$  is the band gap energy, and  $k$  is Boltzmann's constant.

As shown in Figure 13, to decrease the dark current the CCD's must be operated at low temperatures as the dark current generated at room temperature would completely flood the CCD. The average operating temperature of BigBOSS 4k x 4k backside-illuminated CCD's is 140K (W. Kolbe, 2011).

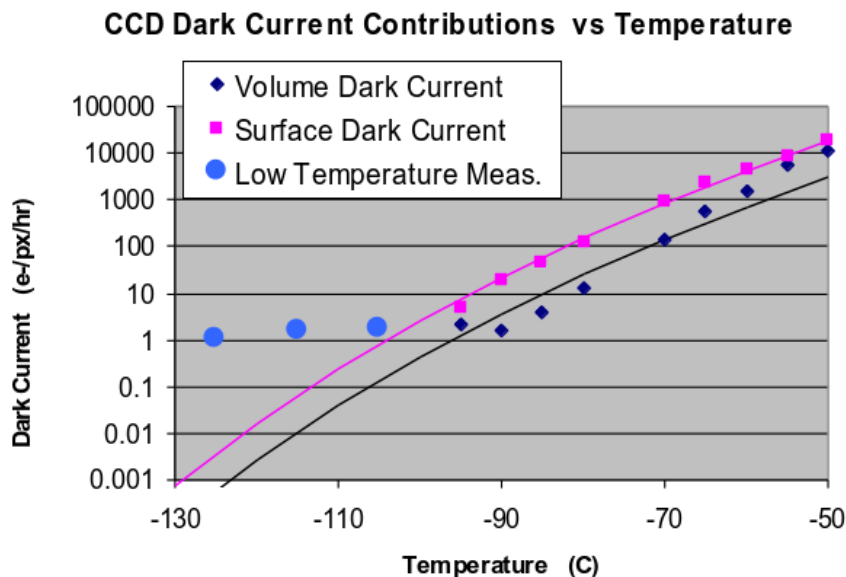


Figure 13: Volume dark current indicates the dark current through the entire bulk of the CCD, and surface dark current refers to the dark current generated on the CCD's surface. Both show the dark current as a function of temperature for BigBOSS CCDs.

### GAIN MEASUREMENTS

Since LBNL produces CCD's for astronomical uses, it's imperative that they perform well in low light conditions, for this reason the CCD's have multiple amplifiers. The amount of amplification is referred to as the gain, and is calculated by finding the ratio between the number of electrons recorded by the CCD and the number of digital units contained in the CCD image. The total signal acquired from the CCD is divided by the gain to ensure that the amount of electrons per pixel used in the QE calculations hasn't been amplified.

The x-ray method of gain measurement is performed by exposing a CCD to an x-ray source that causes a known number of electrons to be emitted when an x-ray event occurs within the silicon. I used  $^{55}\text{Fe}$  for my x-ray measurements:

$$Gain = \frac{ADU}{E_{xray} / E_{e-h}} \quad (9)$$

$ADU$  is the CCD's output signal (analog digital units), which I divided by the ratio of the x-ray and electron hole pair formation energy. Thus, the gain is the total amount of amplification that was applied to the signal by the amplifiers.

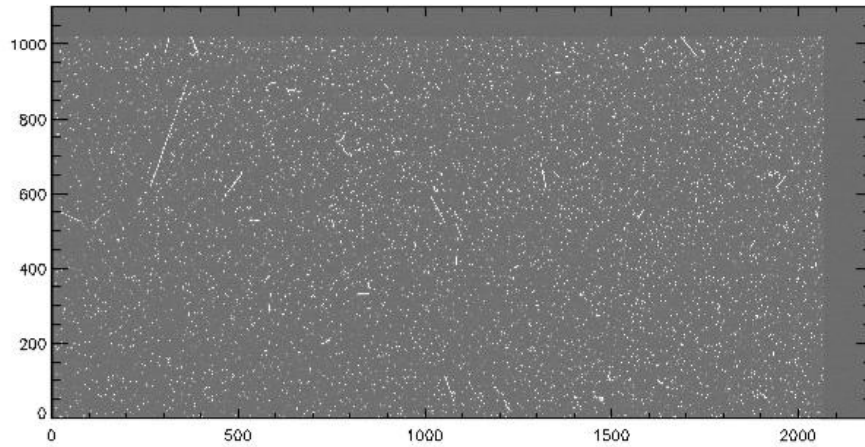


Figure 14: image of x-ray events in a BigBOSS 4k x 2k CCD.

The x-ray events in Figure 14 are detected using LBNL CCD\_Analyze IDL software, which “draws” either a 3x3 or 5x5 pixel box around each pixel whose signal exceeds the user specified sky value of the x-ray image. The summed value is considered to represent the number of electrons that were produced by x-ray events that occurred in the silicon. The reproducibility of this method had been found to be accurate within 0.5% (J. Steckert, 2005).

## CHAPTER 5 QUANTUM EFFICIENCY MEASUREMENTS

### QUANTUM EFFICIENCY VERSUS WAVELENGTH

A CCD's quantum efficiency is dependent on a multitude of factors, including its temperature, the incident light intensity, and wavelength. Since the dependence on temperature and intensity is well known and standard among LBNL backside illuminated CCDs, I kept those parameters uniform in the QE measuring system, with the wavelength dependence as the variable of interest. CCDs are designed to have greater response to the wavelengths that are deemed most vital to the experiment that the CCD is to be used for. Experiments that focus on detecting ultra-violet emitting events require CCDs that are more sensitive in the blue end of the spectrum (about 200nm to about 500nm). Subsequently, experiments that focus on detecting events that emit light of longer wavelengths require CCDs that are more sensitive in the red end of the spectrum (about 600nm to about 1200nm).

As shown in Figure 15, the measured 500um 4k x 2k backside-illuminated CCD (tin 4k x 2k, ID: 145912.4.3) was designed to be sensitive to longer wavelengths. In the blue end of the spectrum the QE is low, indicating that the CCD not very responsive. At about 850nm the response becomes noticeably better, and as such, becomes more temperature dependent, as shown in Figure 16.

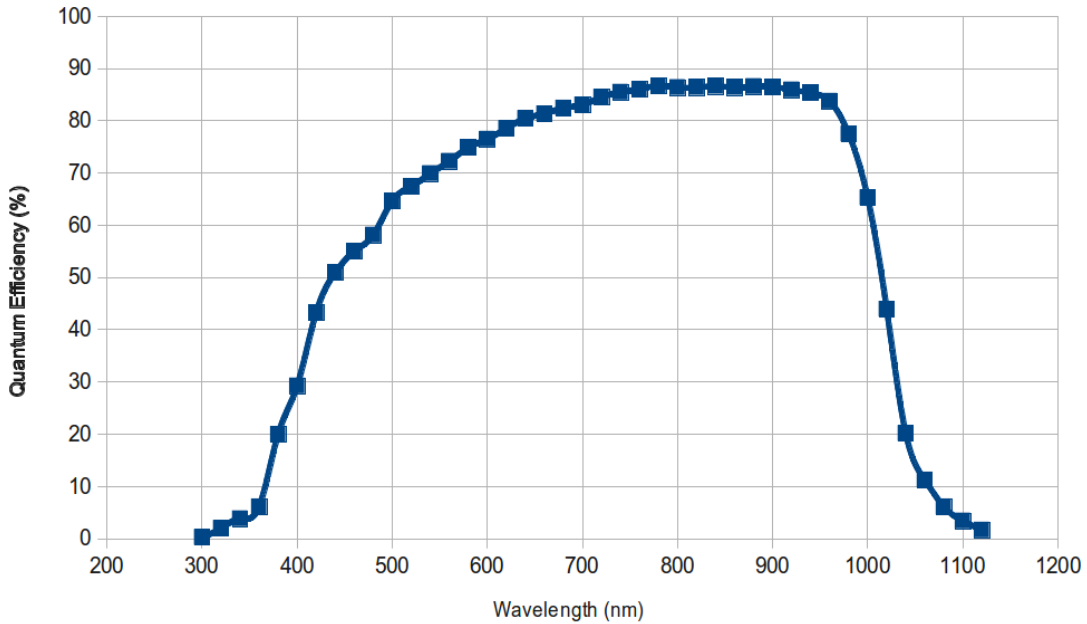


Figure 15: QE versus wavelength of a tin 500um 4k x 2k backside-illuminated CCD (ID#: 145912.4.3) measured at 140K.

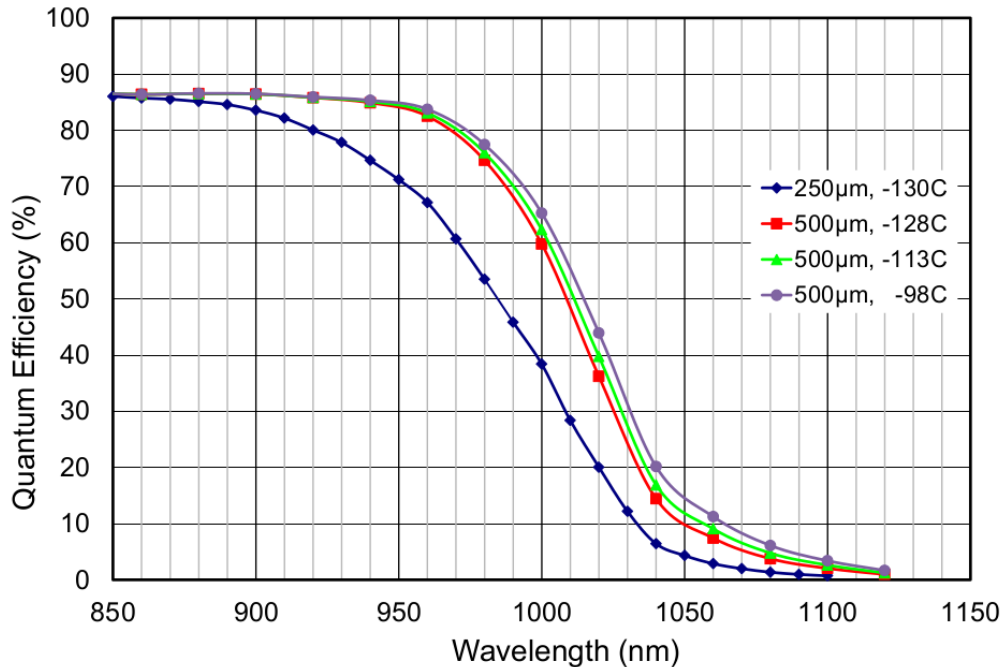


Figure 16: QE versus wavelength of a tin 500um 4k x 2k backside-illuminated CCD (ID#: 145912.4.3). The measurements were repeated at various temperatures to show the temperature dependence of the QE. A 250um CCD is also included to show the dependence on CCD thickness in the red end of the spectrum.

Figure 16 also shows the effect that CCD thickness has on the QE in the red end of the spectrum. QE is partly a function of the thickness of the CCD relative to the absorption length of the incident photons. A photon's absorption length in silicon is proportional to its wavelength. Higher energy photons of shorter wavelengths have shorter absorption lengths. As such, they are either absorbed near the surface of the CCD or are reflected and scattered. Lower energy photons of longer wavelengths have longer absorption lengths and travel farther into the silicon before emitting electrons. If longer wavelength photons are not absorbed, they either pass completely through the silicon or are dispersed into the CCD's architecture and electronics. Therefore, thicker CCDs are more sensitive to light of longer wavelengths as the extra silicon compensates for the photon's extended absorption length. Therefore, the 500um CCD is more responsive to light in the red end of the spectrum than the 250um CCD (C. Bebek, 2012).

### **ANALYSIS SCRIPTS**

I calculate the QE using two different methods depending on which mode the system is run in. Photodiode mode finds the ratio of the total current generated in the CCD for a given wavelength and the total current generated by the photodiode at the same wavelength. When in photodiode mode, the CCD does not take actual images that are read out by the controller.

Unlike photodiode mode, imaging mode uses an LBNL standard fits file analysis package to calculate the electrons generated by analyzing flat field images.

Both modes find the ratio between the number of electrons generated by the CCD and the photons incident on its surface, but since each mode records data in a different form, the analysis routines are different.

Photodiode mode analysis script: my photodiode analysis script calculates the QE for each wavelength by comparing the QE of the photodiode with the currents measured from the CCD:

$$QE_{CCD} = \frac{QE_{photodiode} * [I_{CCD} * C - I_{CCD(dark)} * C]}{I_{photodiode} * C - I_{photodiode(dark)} * C} * \frac{A_{photodiode}}{A_{CCD}} \quad (10)$$

$A_{CCD}$  is the area of the CCD, and  $A_{photodiode}$  is the area of the photodiode in square meters. The QE of the photodiode is divided by the CCD and photodiode currents. I take dark measurements are taken for each wavelength and subtract them from the exposed measurements to help remove the effects of light leaks.

Each current shown in the QE formula is multiplied by the monitoring correction current to account for the possible difference in light level between the photodiode container and CCD Dewar runs, as given in Equation (3).

The QE of the photodiode is multiplied by the CCD current and divided by the photodiode current, which are both adjusted for dark currents, and the resulting value is multiplied by the ratio of the photodiode's area to the CCD's area. The QE of the photodiode was measured by the manufacturer and is shown in Figure 17.

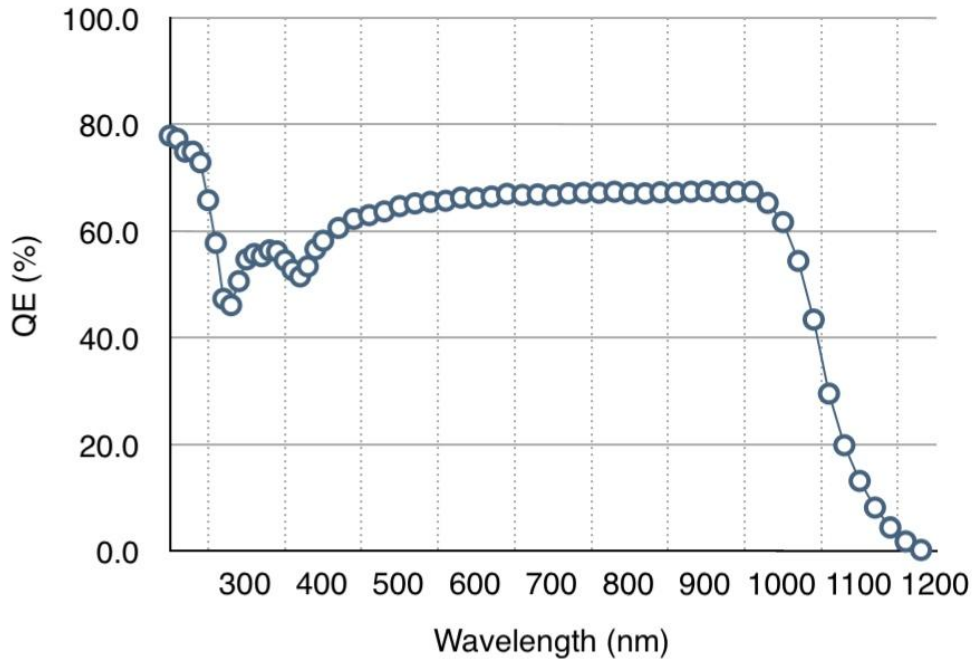


Figure 17: QE versus wavelength of the 10mm photodiode in the photodiode container.

CCD imaging mode analysis script: my imaging mode analysis script calculates the QE by finding the average signal level from the flat field at each wavelength, calculating the number of emitted electrons, and comparing it to the amount of photons detected by the photodiode.

The signal is loaded into a three dimensional array that represents the row and column structure of the CCD. I visually inspect the CCD images and select an area that appears to have no defects or abnormalities, such as hot columns or edge effects, and designate it the "active area". I then calculate the average QE within the bounds of that area.

I subtract the signal taken from the dark images, from the signal taken from the exposed images, and use them to calculate the  $ADU$  per pixel:

$$ADU_{pixel} = Signal_{exposed} - Signal_{dark} \quad (11)$$

This represents the number of electrons emitted and collected for that exposure, including the gain applied by the amplifiers. I divide the  $ADU$  by the gain to remove the effect of the amplification and find the actual number of electrons per pixel:

$$N_{e^-} = \frac{ADU_{pixel}}{Gain} \quad (12)$$

I calculated the gain using equation (9). I then find the number of photons per pixel (photons/pixel/sec) by multiplying the light level  $\rho$  (photons/m<sup>2</sup>/sec) by the CCD's pixel size to find the number of photons:

$$\rho_{pixel} = \rho * A_{pixel} \quad (13)$$

I have calculated  $\rho$  (photons/pixel/sec), using equation (6). I divide the number of electrons per pixel by the exposure time to find the number of electrons per second. Finally, I divide the number of electrons (electrons/pixel/second) by  $\rho_{pixel}$  from equation (13) which gives the average QE of the CCD for the given wavelength:

$$QE_{CCD} = N_{e^-} * \frac{1}{t_{expose}} * \frac{1}{\rho_{pixel}} \quad (14)$$

As with photodiode mode, I apply a monitoring correction current to account of the possible difference in light level between the photodiode container and CCD Dewar runs.

## CHAPTER 6 SYSTEM EQUIPMENT ERROR

The following errors are systematic absolute errors that are independent from the actual measurement. These sources of error are inherent to the equipment used and have been measured by the manufacturers. In the QE setup, these errors contribute a small fraction of the total error and are not noticeable in the QE measurements.

### SHUTTER

The iris shape of the shutter causes the blades to obstruct the beam from the outside inward when it is either opening or closing. The blade contraction process takes 6ms; therefore for 12ms during each exposure the beam is not completely uniform. To compensate for this, the manufacturer recommends that exposures of at least 1.1 seconds be taken to keep the error below 1%. I use an average exposure time between 5 and 20 seconds for all my QE measurements.

According to the manufacturer, given the range of exposure times I use, the opening and closing of the shutter causes the light intensity to deviate by 0.08%. This error is so minimal that it is not considered to be a large influence on light uniformity, and LBNL considers it to be negligible.

### FILTERS

The filters are used to block the higher order effects of the incident light. According to Hoya, the manufacturers of our bandpass filters, the second order light is attenuated by 1000, or an intensity of 0.05% of the first order light. The 0.05% increase in light intensity is generally

out-of-band light that is removed by the monochromator. Therefore, this error created by the filters is considered to be negligible.

### **MONOCHROMATOR**

The largest source of error caused by the monochromator is the relative stray light, which causes 0.75% of the in-band-light to fluctuate or be lost (manufacturer estimate). This is usually caused by the imperfect nature of the mirrors, slits, and grating inside of the monochromator. If the monochromator is unable to correct for the second order light effects, discussed in Chapter 2, then the worst systematic error caused by the monochromator and filters is about 0.8% of the light that is incident on the CCD (J. Steckert, 2005).

### **SPHERE**

The integrating sphere is a passive object in the beam line, and any alteration to the light uniformity is accounted for by the inclusion of the photodiode on its inner surface and the associated monitoring correction current that is applied to the QE. The monitoring correction current shown in Figure 18, is usually less than 2 pico-amps, contributing less than 0.005% deviation in overall light intensity across all wavelengths. 500nm to 800nm is the range that the monochromator operates most efficiently in. From 200nm to 500nm and above 800nm there are fluctuations in the light intensity, though those fluctuations are also less than 2 pico-amps, and thus contribute minimal error.

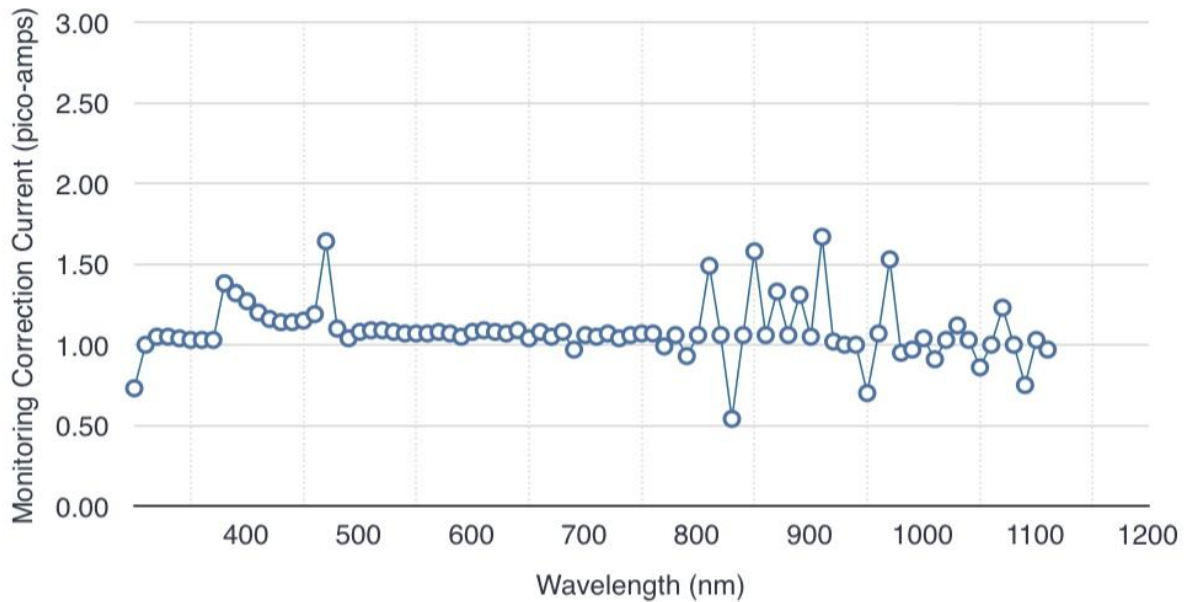


Figure 18: Monitoring correction current versus wavelength. The fluctuations in the monitoring correction current are on the order of pico-amps. Since the measurements are on the order of nano-amps, the error caused by light leaks is negligible.

### LIGHT LEAKS

I calculated the light leaks from the entire system, including the Dewar and photodiode container, by examining a series of dark images. The images showed that the total contribution of light leaks in the system is no more than about 50fA. Since the measurements are on the order of nano-amps, the error caused by light leaks is negligible.

### TOTAL ERROR

The error in the QE is directly related to the fluctuations in the light level. A lack of uniformity in the light intensity causes error in the calculation of photons per pixel calculated in equations (13). Normally, the error to the QE caused by fluctuations in the light intensity is considered by LBNL to be negligible.

The maximum total deviation of the in-band light intensity as estimated by the various equipment manufacturers added in quadrature:

Shutter: 0.08%

Filters: 0.05%

Monochromator: 0.75%

Sphere with monitoring correction current: 0.005%

Total error: 0.756%

To verify this error, LNBL placed a calibrated photodiode in the beam line before the monochromator, took current measurements, and then placed the photodiode inside of the Dewar and took similar measurements. They compared the measurements and found that the light intensity fluctuated by 1.78% between the two locations. Normally however, I have found the fluctuations to be around 1.00%. It's possible that condensation on the CCD's surface accounts for the extra 0.244% average deviation in the light intensity. Condensation on the CCD's surface could be causing some of the incident light to be scattered and therefore not absorbed by the CCD. This is currently being researched at LBNL. To better understand the implication of the 1.00% fluctuation in the light intensity on the QE plots generated from the QE system's measurements, I performed repeated measurements on a single CCD at the same temperature and wavelength range. The resulting plot shows that the 1% light intensity fluctuation has a minimal effect on the QE, as shown in Figure 19.

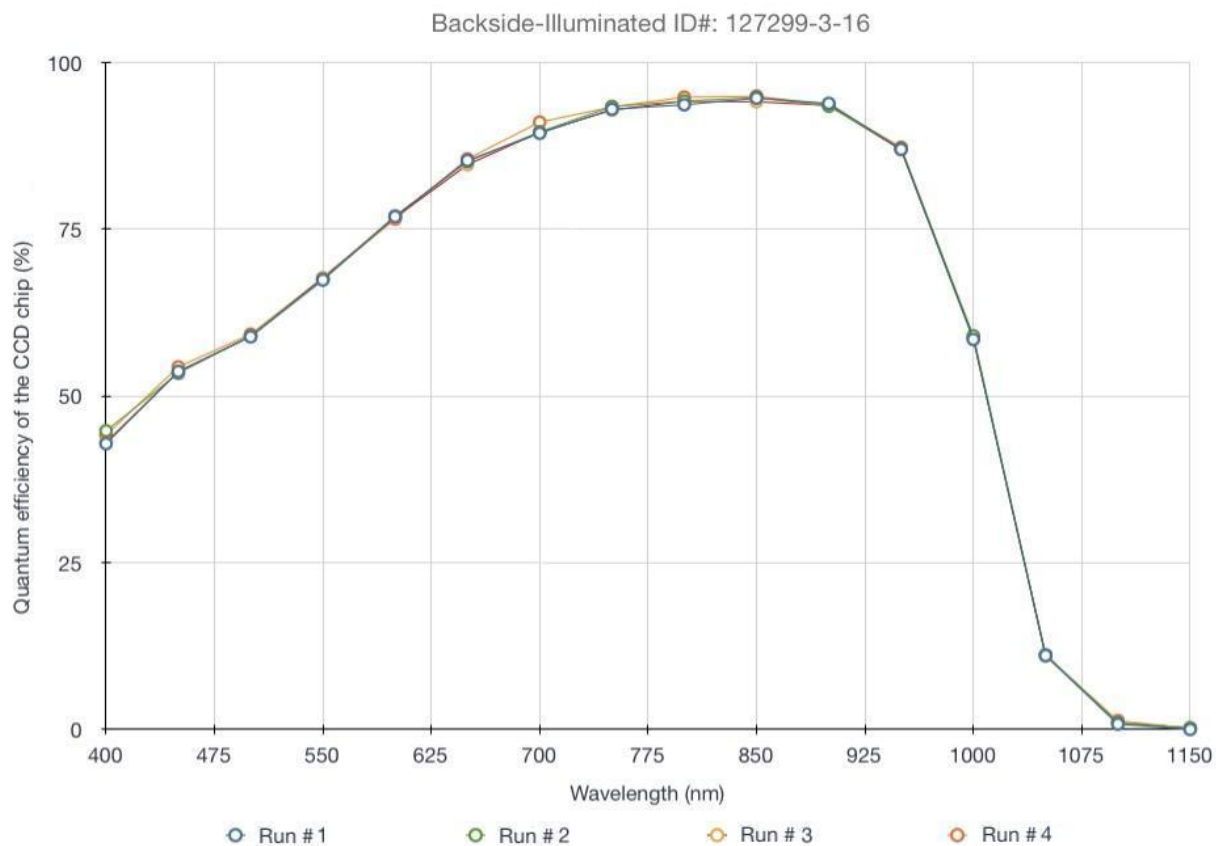


Figure 19: Four sequential measurement runs performed sequentially on a backside-illuminated LBNL CCD (ID#: 127299.3.9). The CCD temperature was held constant at 140K for each run.

The deviations of the QE measurements from the average for each wavelength are shown in Figure 20. Between 400nm and 1050nm the deviation is negligible, however, after 1050nm the deviation increases. The poor sensitivity of the CCD to wavelengths over about 1000nm accounts for the noticeable deviations. This is caused by the architecture of the CCD and was expected.

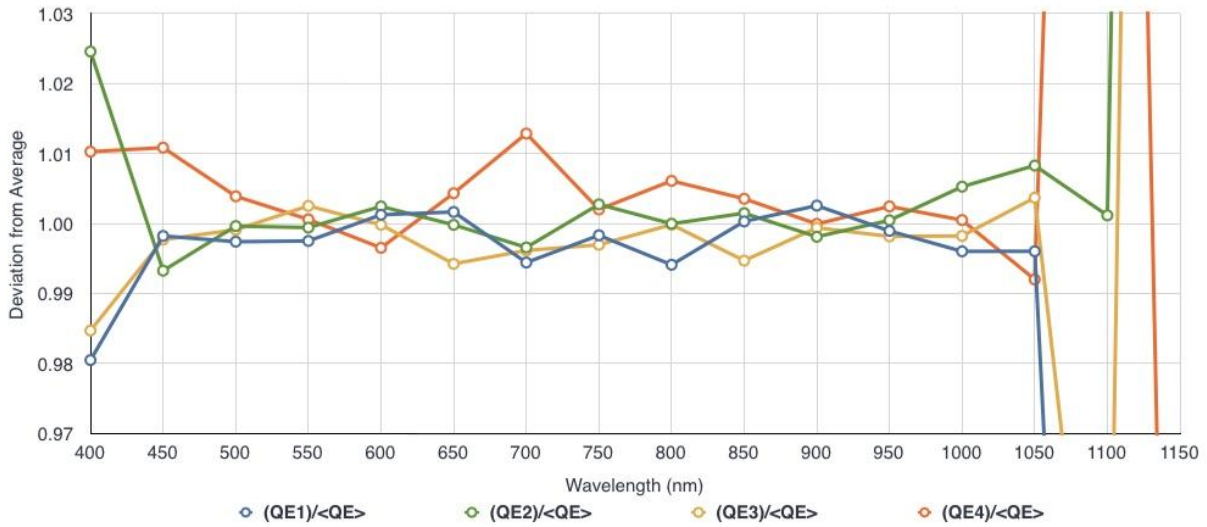


Figure 20: Deviation from the mean QE for four sequential measurement runs performed sequentially on a backside-illuminated LBNL CCD (ID#: 127299.3.9). The CCD temperature was held constant at 140K for each run.

It has been suggested that improved anti-reflective coatings could improve calibration uncertainties, though whether this warrants further research is debatable as the uncertainty caused by the atmospheric conditions that light incident on the CCD would be exposed to is greater than 1% (C. Stubbs, 2006).

## CHAPTER 7 CONCLUSION

The separation of the photodiode from the Dewar did not contribute noticeable error to the LBNL QE measurement system, and has made room for the 4k x 2k and 4k x 4k BigBOSS backside illuminated CCDs. Formerly, the maximum CCD size that the system could accommodate was 2"x2". My alterations now allow CCDs of 3.4"x3.4" or larger to be measured within the QE apparatus.

The uncertainty in the number of calculated photons per pixel caused by fluctuations in the light intensity is estimated by the various hardware manufacturers to be 0.885% of the incident light intensity. However, in practice the fluctuations in light intensity have been measured to be a maximum of 1.78% of the incident light. The possibility that the extra error is caused by condensation forming on the surface of the CCD is currently being researched.

My photodiode container accurately mimics the Dewar's interior in regard to environmental conditions and reflection suppression. The use of the same dewar window for both dewar and container measurements ensures that any effects on the light uniformity caused by the index of refraction and scattering properties of the glass is uniform between container and dewar measurements. To prevent the glass from collecting condensation that would contribute to scattering of the incident light, I constructed a pressurized air system that uniformly blows air onto the window, preventing condensation from forming.

My JAVA scripts automate the system and run the photodiode container and Dewar measurements without need of user assistance. In addition, the system now performs

measurements over a series of temperatures by automatically heating or cooling the CCD after each series of wavelength measurements are completed.

My data analysis scripts combine the data from the photodiode container and CCD to calculate the QE of the CCD in either photodiode or imaging mode. The resulting output file contains all the raw and calculated data from all the wavelengths measured.

My new QE system design succeeds in accommodating large CCD's and is being used to test all the science grade CCD's that will be used in the BigBOSS project as well as future experiments.

**APPENDIX A**

This list covers the major parts used in the QE system (part, model, description):

Xenon Light Source:

Lamp, Oriel 6257, 100W Xenon Lamp.

Socket adapter, Oriel 66150, Lamp Socket adapter.

Lamp Housing, Oriel 66902, 50-500W Arc Housing with F/1 condenser.

F/# matching Lens, Oriel 41575, F/4.6 152mm focal length.

Power Supply, Oriel 68907, Power supply for Arc lamps.

Lens holder, Oriel 6195, Lens holder for 1.5" lenses.

F/4.6 focusing lens, Oriel 41575, UVFS lens.

Stabilization:

Stabilization, Oriel 68950, Light intensity controller system.

Adapter for 66902 housing, Oriel 68855.

Shutter:

Shutter, Uniblitz VS25S2ZM0R1, 25mm aperture Shutter.

Monochromator and Filter Wheel:

Monochromator, Oriel 77700, Ms257 Oriel monochromator.

Multiple Grating Turret, Oriel 77708, Triple grating turret.

Gratings, Oriel 77742, 1200g 350nm blaze.

Oriel 77752 706 1200g 750nm blaze.

Mirror, SP45700-1738, Mirror 50x50x6m, coated one side.

Motor driven Silt assembly, Oriel 77722, Variable input slit.

Slit controller Board, Oriel 77712, Motorized single slit control.

Fixed slit, Oriel 77212, 3.16mm fixed slit.

Output Mirror, Oriel 77716, Motorized flip output mirror.

Motorized Filter Wheel, Oriel 77737.

Dielectric filters:

Bandpass, Hoya U340 FSR-U340

Bandpass, 466FCS2500 Schott BG23

Longpass, FLWP-450-25.0m

Longpass, FLWP-700-25.0m

Integrating Sphere:

Integrating Sphere, LabSphere CSTM US2000, 20" Integrating Sphere.

**Light Measurement:**

Photo Diode, Hamamatsu S1337-1010BQ, Calibrated Photo Diode.

Photo Diode, Hamamatsu S2281, Calibrated Photo Diode.

Picoammeter, Keithley 6485, Picoammeter for Diode Readout (x2).

Optical Table, Newport IG-35-2, 90x150 cm.

Breadboard, Newport IG-36-2, 90x180 cm Breadboard.

Temperature monitor, Lakeshore 321 auto-tuning (x2).

**Automation:**

Linux PC + monitor, PC compatible with the leach controller board.

Serial board, DIGI Neo Classic 8, 8-port RS232 board.

Breakout cable, Opt8-M9, 8-port DB9 breakout cable.

**APPENDIX B**

These are the schematics for the construction of the photodiode container:

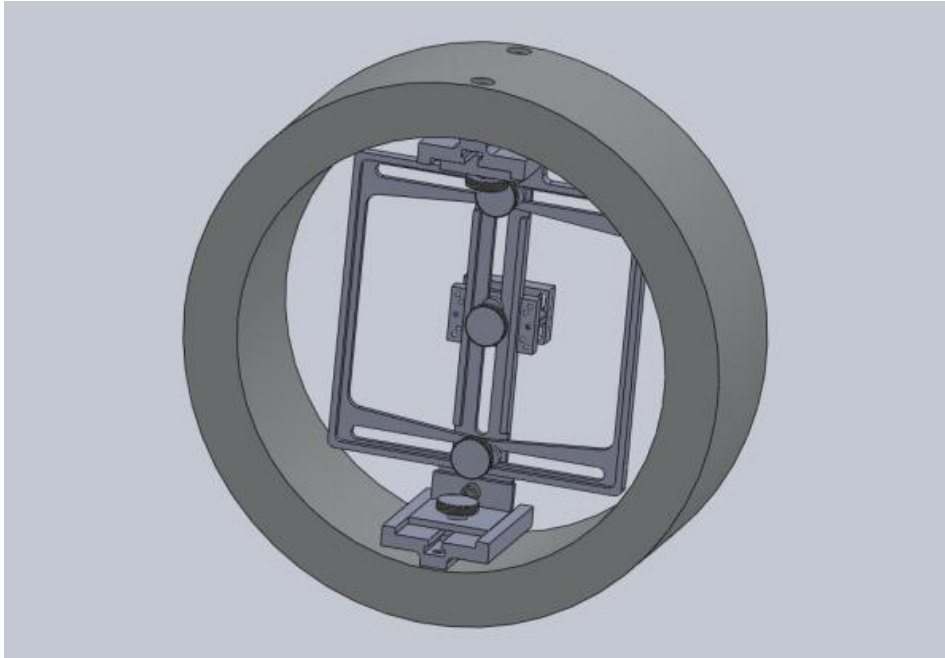


Figure 21: back assembly.

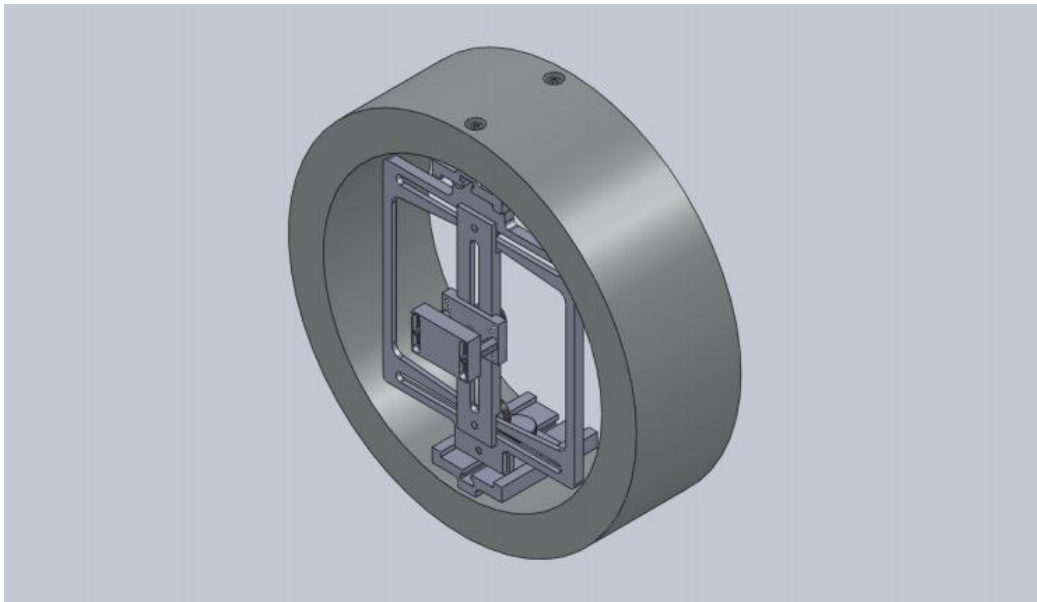


Figure 22: front assembly.

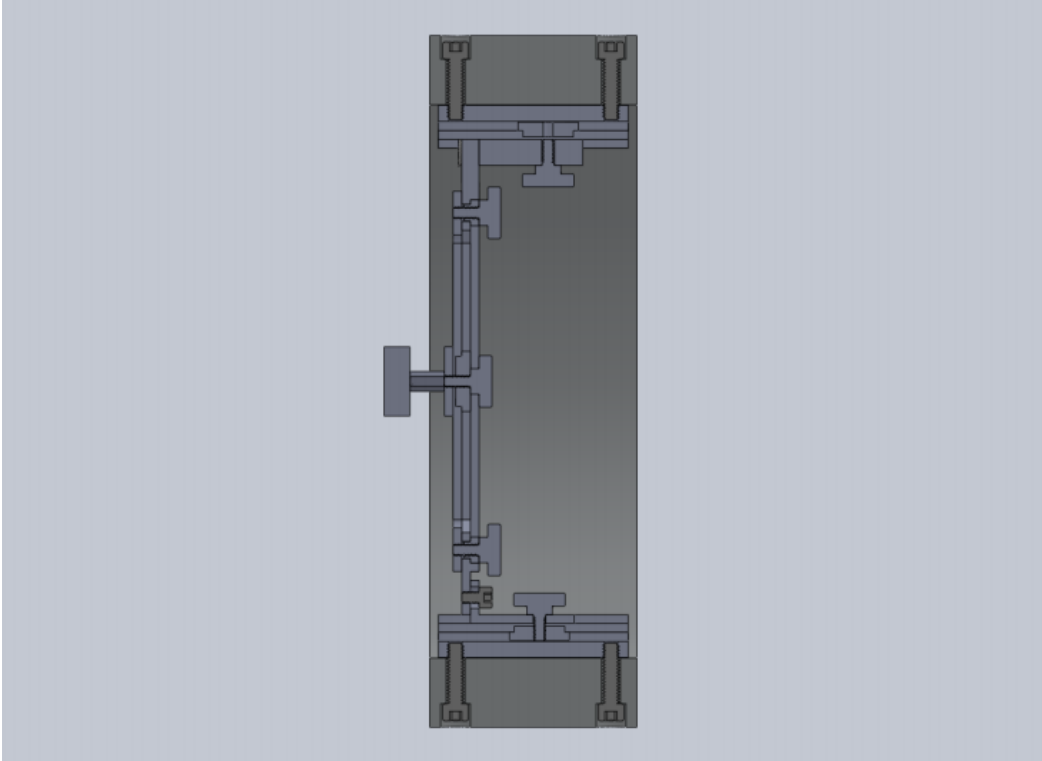


Figure 23: cross section assembly.

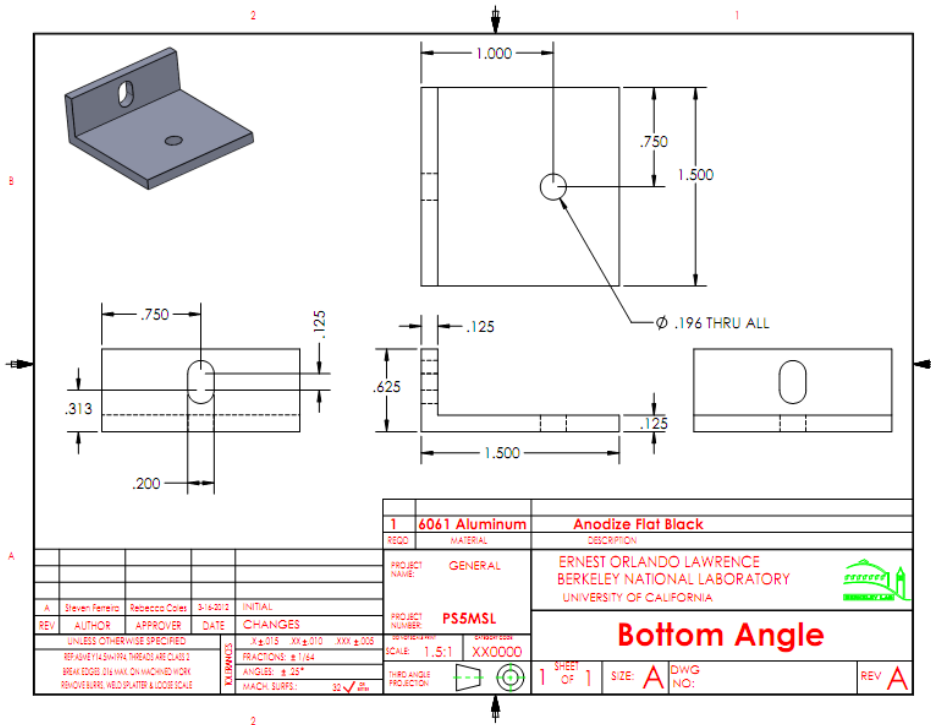


Figure 24: bottom angle.

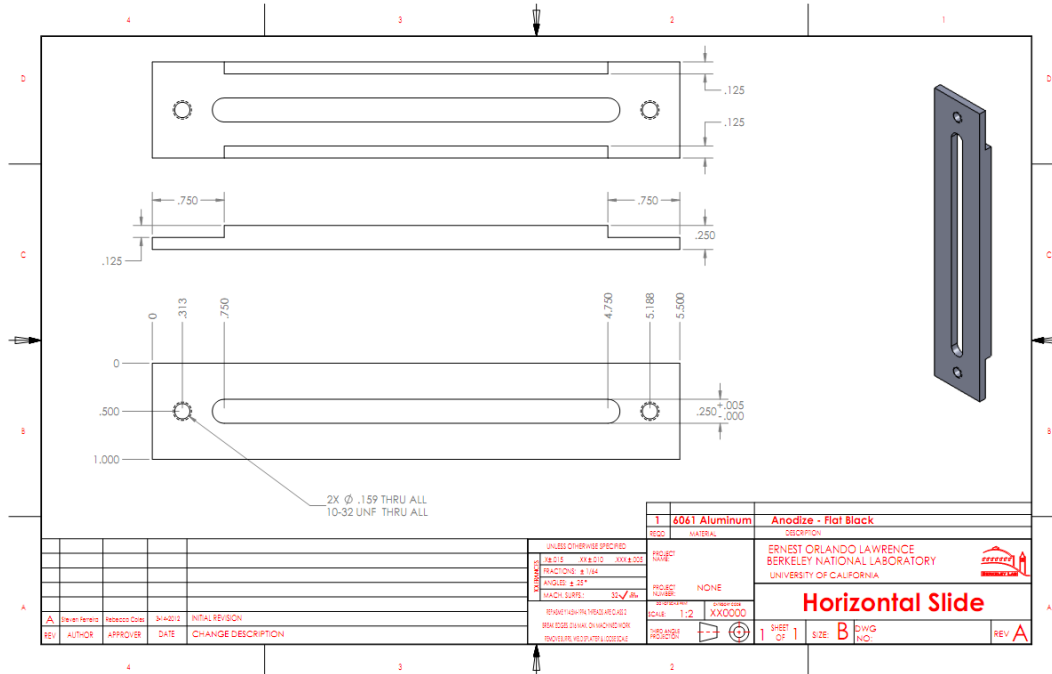


Figure 25: horizontal slide.

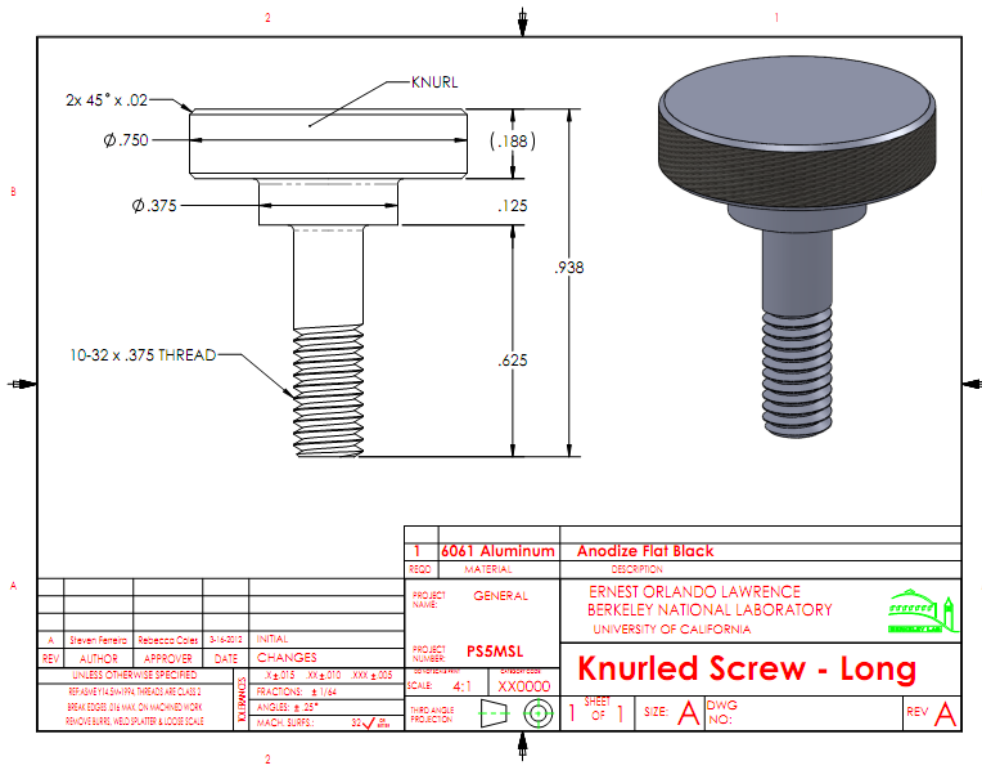


Figure 26: long knurled screw.



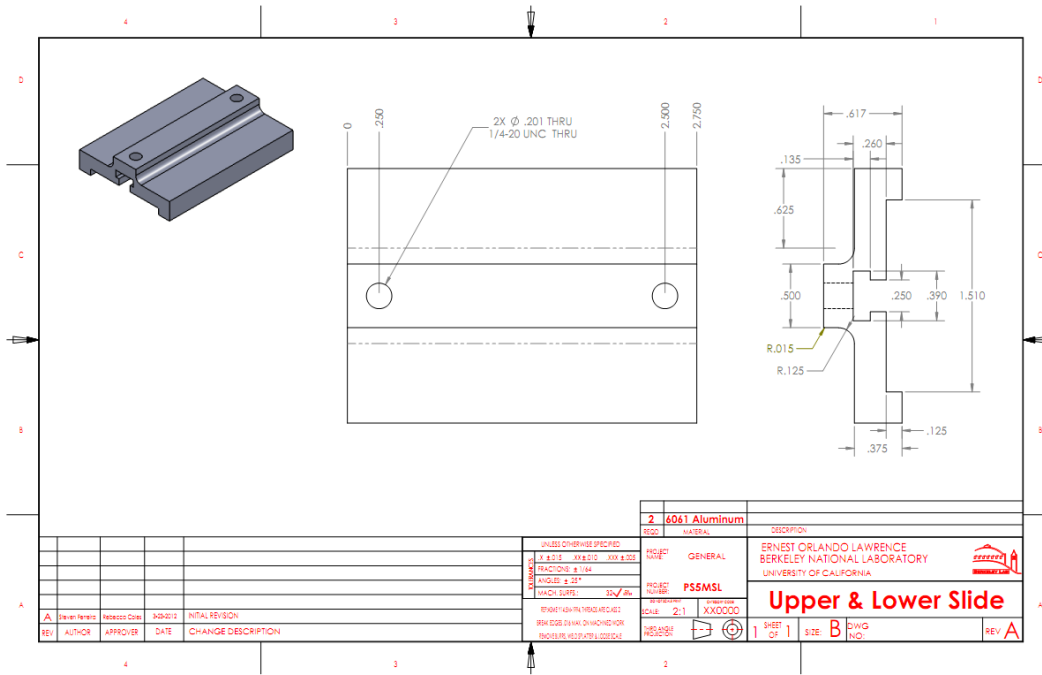


Figure 29: upper and lower slide.

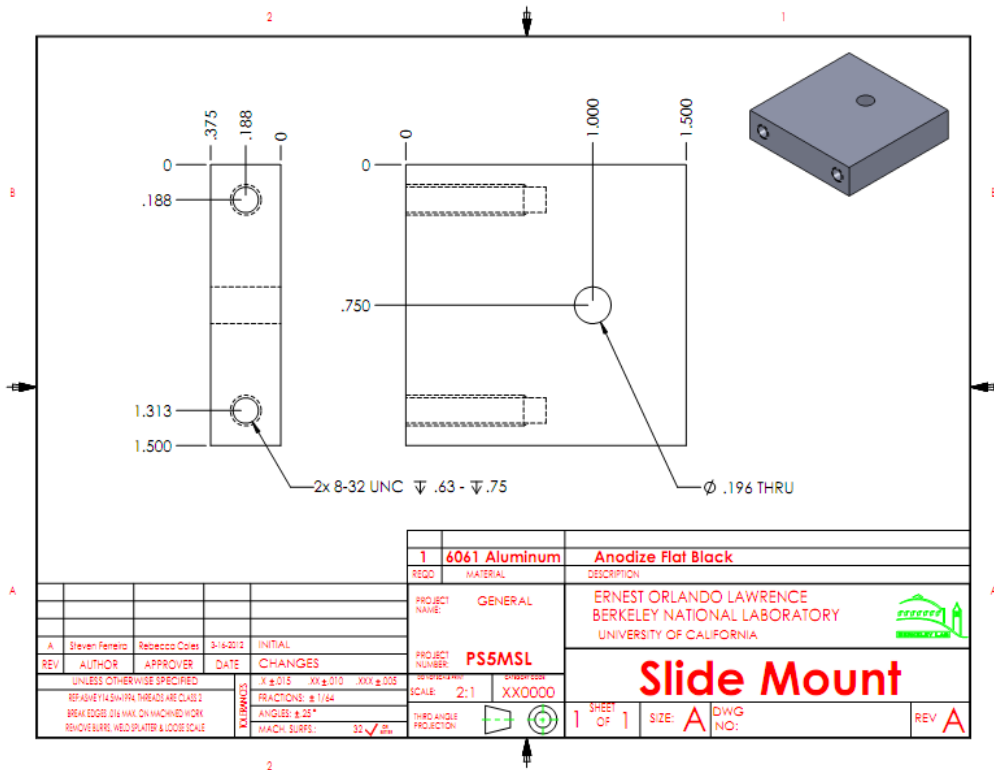


Figure 30: slide mount.

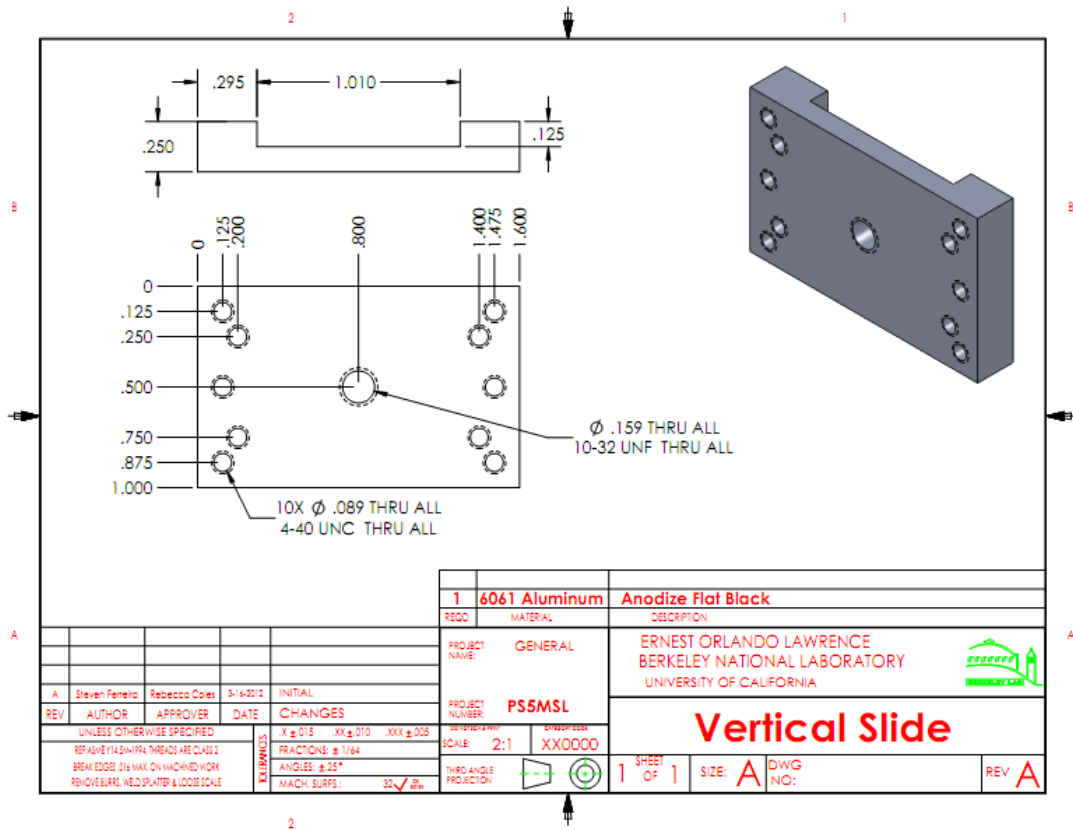


Figure 31: vertical slide.

**REFERENCES**

- Janesick, J. 2001, *Scientific Charge Coupled Devices*, The International Society for Optical Engineering
- Steckert, J. 2005, Design, implementation and setup of an automated quantum efficiency measurement system for charge-coupled devices, Unpublished diploma thesis, **81**, 82
- Kolbe, W. 2011, Dark Current in BigBOSS CCDs, Unpublished LBNL research.
- Stubbs, C. 2006, Toward 1% Photometry: End-to-end Calibration of Astronomical Telescopes and Detectors, *Astrophys.J.*646: 1436-1444
- Bebek, C. 2012. With R.A. Coles, P. Denes, F. Dion, J.H. Emes, R. Frost, D.E. Groom, R. Groulx, S. Haque, S.E. Holland, A. Karcher, W.F. Kolbe, J.S. Lee, N.P. Palaio, N.A. Roe, C.H. Tran, and G. Wang, CCD Research and Development at Lawrence Berkeley National Laboratory, 8453-04 SPIE, **4**
- Lawrence Berkeley National Laboratory and The National Optical Astronomy Observatory, 2009, BigBOSS: The Ground-Based Stage IV BAO Experiment (White Paper), Retrieved from: <http://arxiv.org/abs/0904.04>

**ABSTRACT****AN APPARATUS FOR VERIFICATION OF ABSOLUTE CALIBRATION OF QUANTUM EFFICIENCY FOR CHARGE-COUPLED DEVICES**

by

**REBECCA COLES****December 2012****Advisor:** Professor David Cinabro**Major:** Physics**Degree:** Master of Physics

The LBNL Microsystems Laboratory produces backside illuminated, high resistivity, p-channel, charge-coupled devices (CCDs). A system was developed to test the quantum efficiency (QE) of the CCDs; the percentage of electrons that are emitted from the CCD surface per amount of light that it's exposed to.

The QE system was designed and constructed to test CCDs of a much smaller size than what is currently produced. To continue testing, I redesigned the QE apparatus to make room for the new, larger size, CCDs while still preserving measurement accuracy. I removed the photodiode that formally sat alongside the CCD in the Dewar, and installed it in a separate container. Instead of the CCD and the photodiode taking flux measurements simultaneously, the processes are now performed separately. The error caused by the separation has remained less than 1.78%.

**AUTOBIOGRAPHICAL STATEMENT**

**Name:** Rebecca Coles

**Education:**

B.S. of Physics (Physics & Astronomy), Wayne State University,

Detroit, Michigan, 2008

I entered my college career knowing that my interests lie in science and technology. After I acquired a B.S. in physics, I worked at the Fermi Particle Acceleration Laboratory where I learned that to be an experimental physicist; one had to also be a competent computer programmer, engineer, and mathematician. This knowledge encouraged me to further not only my education in physics but in other sciences as well.

The support of my advisor, David Cinabro, and the staff at the Lawrence Berkeley National Laboratory has allowed me to improve my skills as both a researcher and a student.